HSR (LONDON),
HOUGHTON STREET REVIEW JOURNAL
ISSN: 2058-5519|Impact factor-15.9
http://houghtonstreetreview.com/index.php/hsr

# URBACH ENERGY AND $sp^2$ CLUSTER STRUCTURE OF GRAPHENE OXIDE AS BASELINE PARAMETERS FOR INTERPRETING MAGNETO-OPTICAL SPECTRA OF GO/$Fe_3O_4$ HYBRIDS

**R.Sh. Daminov[1], Z.Z. Ne'matova[1], M.S. Bozorova[1]**

[1] National University of Uzbekistan named after Mirzo Ulugbek, Center for the Development of Nanotechnologies, Tashkent, Uzbekistan

guliston.92@gmail.com

Doi: https://doi.org/10.5281/zenodo.23161887

**Abstract.** The optical absorption edge of graphene oxide (GO) synthesized by the Hummers method was analyzed using UV-Vis spectra of aqueous dispersions. The ln α versus hν dependence is linear over 2.00–3.45 eV ($R^2$ = 0.9994), giving an Urbach energy $E_U$ = 0.91 ± 0.01 eV that does not depend on concentration. Tauc fits with n = 2 and n = 1/2 are of equal quality and yield $E_g$ = 3.35 eV and 1.87 eV, respectively. From the Raman intensity ratio $I_D/I_G$ = 0.83, the Ferrari–Robertson model gives a characteristic $sp^2$ cluster size $L_a \approx 1.2$ nm, which by the Robertson–O'Reilly relation corresponds to $E_g \approx 1.3$ eV and is therefore closer to the n = 1/2 result than to the n = 2 result. The ratio $E_U/E_g$ = 0.27 and the Urbach steepness parameter σ = 0.028 confirm the strongly disordered structure of GO. The obtained parameters are proposed as a baseline for interpreting magnetic circular dichroism (MCD) and Kerr spectra of GO/$Fe_3O_4$ hybrids, and a scheme for distinguishing two mechanisms is presented.

**Keywords.** graphene oxide, Urbach energy, Tauc analysis, $sp^2$ cluster, Raman spectroscopy, magnetic circular dichroism, $Fe_3O_4$.

## 1. Introduction

Hybrid systems in which magnetite ($Fe_3O_4$) nanoparticles are anchored to graphene oxide (GO) are widely studied for catalysis, sensing and magnetic materials [1]. The magneto-optical response of such systems, in particular magnetic circular dichroism (MCD) and the Kerr effect, is closely linked to the shape of the absorption spectrum. The A-term of the MCD spectrum is proportional to the energy derivative of the absorption band, while the Kerr rotation and ellipticity are related through the Kramers–Kronig relations to the off-diagonal component of the dielectric tensor [2]. In the magneto-optical spectra of $Fe_3O_4$, charge-transfer and crystal-field transitions involving $Fe^{3+}$ and $Fe^{2+}$ ions at tetrahedral (A) and octahedral (B) sites are observed in the visible and near-ultraviolet region [3].

In a GO/$Fe_3O_4$ hybrid the $Fe_3O_4$ particles are embedded in the GO matrix, so the measured spectrum is the sum of the contributions of the two components. GO itself is a disordered material composed of $sp^2$ and $sp^3$ hybridized carbon domains, and its optical properties are governed by $\pi \leftrightarrow \pi^*$ transitions in small $sp^2$ clusters [4]. As the degree of oxidation increases, the $sp^2$ clusters shrink and the optical band gap widens [5]. The band gap of GO is usually determined by the Tauc method [6], but in disordered materials the ambiguity in choosing the transition type and the background absorption strongly affect the result [7].

HSR (LONDON),
HOUGHTON STREET REVIEW JOURNAL
ISSN: 2058-5519|Impact factor-15.9
http://houghtonstreetreview.com/index.php/hsr

Below the absorption edge the absorption coefficient decays exponentially, and this region is described by the Urbach rule [8]. The Urbach energy $E_U$ represents the width of the tail of localized states and is accepted as a measure of structural disorder in amorphous semiconductors [9, 10]. From the magneto-optical point of view $E_U$ is particularly important, because the band tail produces absorption inside the band gap and forms a background in the energy range where the $Fe_3O_4$ transitions are located. Most studies of GO focus on $E_g$, whereas $E_U$ is analyzed far less often.

A previous Tauc analysis of Hummers GO prepared in our laboratory gave $E_g$ = 3.34 eV. The aim of the present work is to characterize the absorption edge of the same sample completely, namely to determine $E_U$, to test its stability with respect to concentration and light scattering, to evaluate the Tauc model independently using Raman data, and to develop a scheme for applying the obtained parameters in magneto-optical studies of GO/$Fe_3O_4$ systems.

## 2. Materials and methods

### *2.1. Synthesis of GO*

GO was synthesized by a modified Hummers method [11]. A mixture of natural graphite and $NaNO_3$ was stirred in 98 % $H_2SO_4$ in an ice bath (T < 5 °C). $KMnO_4$ was added in small portions over 6 h while keeping the temperature below 20 °C. The reaction was terminated by adding $H_2O_2$. The precipitate was washed with 1 M HCl and distilled water by centrifugation (8000 rpm) and dried at 50 °C for 24 h.

### *2.2. Characterization*

UV-Vis spectra were recorded on a Shimadzu UV-1900i spectrophotometer in a quartz cuvette (l = 1 cm) in the range 200–600 nm. Measurements were carried out on aqueous dispersions with concentrations of 0.01, 0.08 and 0.12 mg·mL$^{-1}$. The π→π* maximum was determined at all three concentrations, and the absorption edge was analyzed for the 0.08 and 0.12 mg·mL$^{-1}$ samples. Raman spectra were recorded with a 532 nm laser. The elemental composition was determined by energy-dispersive X-ray spectroscopy (EDS).

### *2.3. Calculation methods*

The absorption coefficient was calculated as

$$\alpha=\frac{2.303A}{l} \quad (1)$$

where A is the absorbance and l is the optical path length. The Urbach energy was obtained from the Urbach rule

$$\alpha(h\nu)=\alpha_0 \exp\left(\frac{h\nu}{E_U}\right) \quad (2)$$

as the reciprocal slope of the linear region of the ln α versus hν plot. The band gap was estimated from the Tauc equation

$$(\alpha h\nu)^n=B\left(h\nu-E_g\right) \quad (3)$$

HSR (LONDON),
HOUGHTON STREET REVIEW JOURNAL
ISSN: 2058-5519|Impact factor-15.9
http://houghtonstreetreview.com/index.php/hsr

for n = 2 (direct allowed transition) and n = 1/2 (indirect transition). All linear regions were selected automatically using the criterion $R^2 > 0.999$. To assess the scattering contribution, the exponential model (2) was compared in the range 2.2–3.3 eV with a power-law scattering model $A \propto \lambda^{-n}$. The Urbach steepness parameter was calculated at T = 298 K as

$$\sigma = \frac{k_B T}{E_U} \tag{4}$$

The relation between the optical band gap and the number of aromatic rings M in an $sp^2$ cluster was estimated with the Robertson–O'Reilly relation [12]

$$E_g \approx \frac{6}{\sqrt{M}} \text{ eV} \tag{5}$$

The cluster diameter was obtained from

$$L = 2\sqrt{\frac{MS_0}{\pi}} \tag{6}$$

where $S_0$ is the area of one hexagonal ring

$$S_0 = \frac{3\sqrt{3}}{2} a^2 \tag{7}$$

and a = 1.42 Å is the C–C bond length, which gives $S_0$ = 5.24 $Å^2$. The cluster size was determined from the Raman data using the Ferrari–Robertson model [13]

$$\frac{I_D}{I_G} = C'(\lambda) L_a^2 \tag{8}$$

where the constant C′(λ) is related to the coefficient C(λ) of the Tuinstra–Koenig relation [14] by continuity at $L_a$ = 20 Å [13]

$$C'(\lambda) = \frac{C(\lambda)}{(20\ Å)^3} \tag{9}$$

$$C(\lambda) = -126\ Å + 0.033\lambda \tag{10}$$

with λ expressed in Å. For λ = 532 nm this gives C = 49.6 Å and C′ = 0.0062 $Å^{-2}$.

## 3. Results

### *3.1. General features of the UV-Vis spectra*

At all three concentrations an absorption maximum was observed at 230.5 nm (5.38 eV), which corresponds to the π→π* transition in aromatic C=C bonds [15]. A shoulder at 300–310 nm (4.00–4.13 eV) attributed to the n→π* transition of C=O groups was also observed [15, 16]. The independence of the maximum position from concentration indicates that aggregation effects in the dispersion are weak.

### *3.2. Urbach analysis*

Figure 1a shows the ln α versus hν dependence. It is linear over 2.00–3.45 eV, i.e. over a 1.45 eV wide region, with $R^2$ = 0.9994. Using Eq. (2), $E_U$ = 0.919 eV (0.08 mg·$mL^{-1}$) and 0.904 eV (0.12 mg·$mL^{-1}$) were obtained, with a mean value of $E_U$ = 0.91 ± 0.01 eV. The relative difference between

HSR (LONDON),
HOUGHTON STREET REVIEW JOURNAL
ISSN: 2058-5519|Impact factor-15.9
http://houghtonstreetreview.com/index.php/hsr

the two concentrations is 1.6 %. The fact that $E_U$ remains practically unchanged when the concentration increases by a factor of 1.5 shows that it is an intrinsic property of the material. In the narrow near-edge window (2.80–3.40 eV) $E_U$ = 0.96–0.98 eV was obtained, which is 5.5–7.7 % higher than the main value. Hence the result depends only weakly on the choice of the linear window.

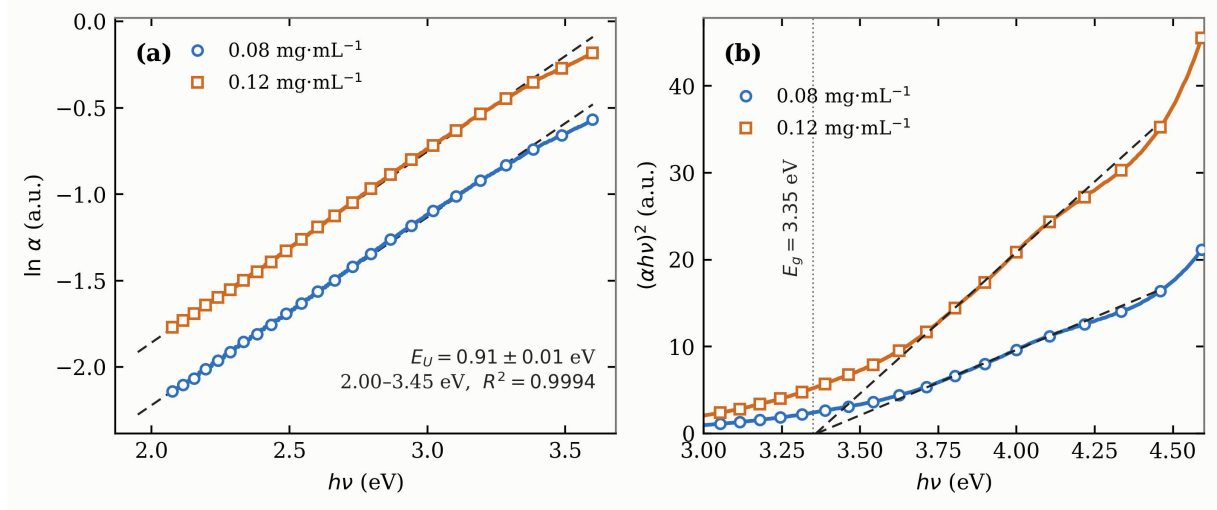



**Figure 1.** (a) Urbach plot ln α versus hν and its linear fit in the 2.00–3.45 eV range. (b) Tauc plot $(\alpha h\nu)^2$ versus hν for a direct transition and extrapolation of the linear region to the energy axis.

### *3.3. Test for the scattering contribution*

Light scattering in a dispersion also produces a background that varies monotonically at low energies and may resemble an Urbach tail. Therefore two models were compared in the range 2.2–3.3 eV. The exponential model gave $R^2$ = 0.99960, and the power-law scattering model gave $R^2$ = 0.99786. The residual variance ($1 - R^2$) of the exponential model is 5.4 times smaller. This indicates that the exponential model is preferable, but since both $R^2$ values exceed 0.997, the scattering contribution cannot be ruled out completely. For this reason the obtained $E_U$ is interpreted below as an effective tail width.

### *3.4. Tauc analysis*

The $(\alpha h\nu)^2$ versus hν plot (Fig. 1b) gave $E_g$ = 3.36 eV in the 3.70–4.15 eV window and $E_g$ = 3.35 eV in the 3.70–4.00 eV window used previously. These values agree with the earlier result of 3.34 eV within 0.01–0.02 eV. The n = 1/2 model gave $E_g$ = 1.87 eV in the range 3.45–4.05 eV with $R^2$ = 0.9992. The fact that both models give fits of practically the same quality shows that the Tauc plot alone cannot determine the transition type unambiguously [7]. This issue is discussed in Section 4.2 using the Raman data. All optical parameters are summarized in Table 1.

HSR (LONDON),
HOUGHTON STREET REVIEW JOURNAL
ISSN: 2058-5519|Impact factor-15.9
http://houghtonstreetreview.com/index.php/hsr

**Table 1.** Optical parameters of GO

| Parameter | Value | Window, eV | $R^2$ |
|---|---|---|---|
| Urbach energy, $E_U$ | 0.91 ± 0.01 eV | 2.00–3.45 | 0.9994 |
| $E_U$ (near-edge window) | 0.96–0.98 eV | 2.80–3.40 | 0.999 |
| $E_g$ (Tauc, n = 2) | 3.36 eV | 3.70–4.15 | > 0.999 |
| $E_g$ (Tauc, n = 2, previous window) | 3.35 eV | 3.70–4.00 | > 0.999 |
| $E_g$ (Tauc, n = 1/2) | 1.87 eV | 3.45–4.05 | 0.9992 |
| π→π* maximum | 230.5 nm (5.38 eV) | | |
| n→π* shoulder | 300–310 nm | | |

### *3.5. Parameters derived from the Urbach energy*

Table 2 lists the quantities derived from $E_U$. At T = 298 K, $k_BT$ = 25.7 meV, and Eq. (4) gives σ = 0.028. Within the 2.00–3.45 eV linear window the absorption coefficient changes by a factor of $\exp(\Delta E/E_U) \approx 4.9$. The ratio $E_U/E_g$ is 0.27 for the n = 2 model.

**Table 2.** Parameters derived from the Urbach energy (T = 298 K)

| Parameter | 0.08 mg·mL$^{-1}$ | 0.12 mg·mL$^{-1}$ | Mean |
|---|---|---|---|
| $E_U$, eV | 0.919 | 0.904 | 0.91 |
| $\sigma = k_BT/E_U$ | 0.0279 | 0.0284 | 0.0282 |
| $\exp(1.45\ \text{eV}/E_U)$ | 4.84 | 4.97 | 4.92 |
| $E_U/E_g$ ($E_g$ = 3.35 eV) | 0.274 | 0.270 | 0.272 |

### *3.6. $sp^2$ cluster size from Raman and EDS data*

The Raman intensity ratio of the D and G bands is $I_D/I_G$ = 0.83, and no 2D band was observed. The upshift of the G band to about 1609 cm$^{-1}$ and the absence of the 2D band indicate that GO belongs to the second stage of the amorphization trajectory, i.e. the transition from nanocrystalline graphite to amorphous carbon [13]. The Tuinstra–Koenig relation is not applicable in this stage, therefore $L_a$ was calculated with Eq. (8), giving $L_a$ = 1.16 nm. For comparison, the Tuinstra–Koenig relation would give $L_a$ = 6.0 nm, which is inconsistent with the absence of the 2D band. According to EDS, C/O = 1.54, i.e. O/C = 0.65, and the oxygen fraction is 39.4 at.% when only C and O are taken into account. This corresponds to a high degree of oxidation [16, 17]. The cluster sizes obtained by three independent approaches are compared in Table 3.

HSR (LONDON),
HOUGHTON STREET REVIEW JOURNAL
ISSN: 2058-5519|Impact factor-15.9
http://houghtonstreetreview.com/index.php/hsr

**Table 3.** Estimates of the $sp^2$ cluster size by different approaches

| Approach | Input quantity | M | L, nm | $E_g$, eV |
|---|---|---|---|---|
| Tauc n = 2 and Eq. (5) | $E_g$ = 3.35 eV | 3.2 | 0.46 | 3.35 |
| Tauc n = 1/2 and Eq. (5) | $E_g$ = 1.87 eV | 10.3 | 0.83 | 1.87 |
| Raman Eq. (8) and Eq. (5) | $I_D/I_G$ = 0.83 | 20.1 | 1.16 | 1.34 |

## 4. Discussion

### *4.1. Degree of disorder and nature of the Urbach tail*

The value $E_U$ = 0.91 eV is much larger than the values typical of crystalline and even amorphous semiconductors. For example, in hydrogenated amorphous silicon $E_U$ is about 0.05 eV [9]. The curves calculated with model (2) in Fig. 2a illustrate this difference clearly. At $E_U$ = 0.05 eV the absorption decreases by six orders of magnitude 0.7 eV below $E_g$, whereas at $E_U$ = 0.91 eV the decrease is only about a factor of two. Hence the density of states inside the band gap of GO is very high. The main reason is the broad size distribution of the $sp^2$ clusters. According to Eq. (5) the gap of each cluster depends on its size, so the sum of contributions from clusters of different size produces a broad absorption tail [4, 12]. The ratio $E_U/E_g$ = 0.27 and the value σ = 0.028 also point to strong disorder, since in ordered crystals σ is typically an order of magnitude higher [10].

At the same time, it should be taken into account that α changes by only a factor of 4.9 within the linear window (Table 2). In a classical Urbach analysis the linear region usually spans several orders of magnitude. It is therefore more appropriate to regard the obtained $E_U$ not as the classical temperature-dependent Urbach parameter but as an effective disorder parameter of GO. Measuring the temperature dependence of $E_U$ would allow this question to be resolved.

HSR (LONDON),
HOUGHTON STREET REVIEW JOURNAL
ISSN: 2058-5519|Impact factor-15.9
http://houghtonstreetreview.com/index.php/hsr

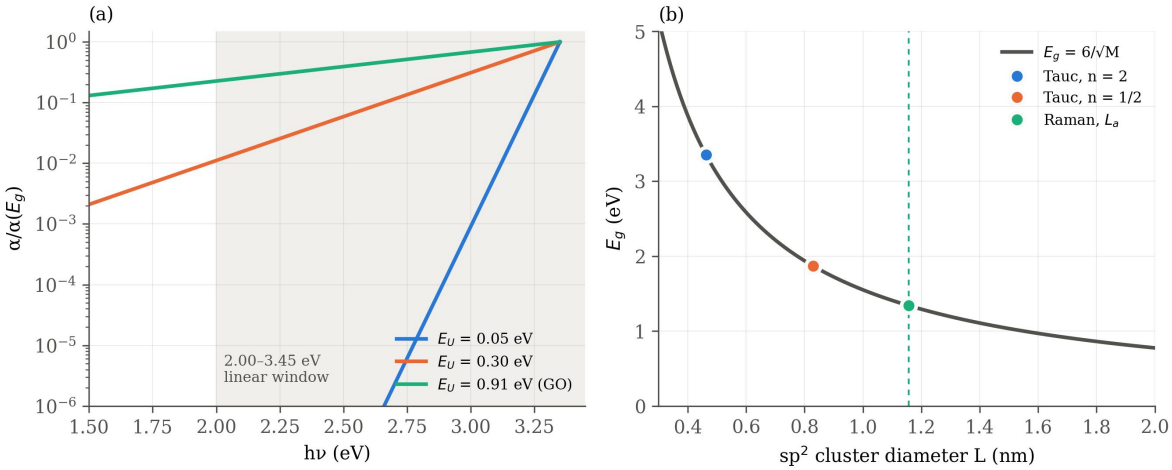



**Figure 2.** (a) Normalized absorption tails calculated with model (2) for $E_g$ = 3.35 eV and three values of $E_U$. The shaded area marks the linear window for GO. (b) Dependence of $E_g$ on sp² cluster diameter according to Eq. (5) and the estimates from Table 3. The dashed line marks the Raman-based $L_a$.

### *4.2. Choice of the transition type*

Figure 2b shows the dependence of $E_g$ on cluster diameter according to Eq. (5), together with the three estimates from Table 3. The value $E_g$ = 3.35 eV from the n = 2 model corresponds to a cluster of only 3.2 aromatic rings with a diameter of 0.46 nm, while the n = 1/2 model gives a cluster of 0.83 nm. The value $L_a$ = 1.16 nm obtained independently from Raman data is closer to the n = 1/2 estimate, since by Eq. (5) it corresponds to $E_g \approx 1.3$ eV. In addition, the model originally proposed by Tauc for amorphous semiconductors has exactly the $(\alpha h\nu)^{1/2}$ form [6]. Thus both the Raman estimate and the theoretical basis support the n = 1/2 model.

However, Eq. (5) is only approximate. Moreover, the 3.70–4.15 eV Tauc window lies in the high-energy part of the spectrum and mainly reflects the contribution of the smallest clusters, whereas the Raman method gives an average size. Therefore both $E_g$ values are retained for further comparisons and are regarded as two limits of the cluster size distribution.

### *4.3. Implications for magneto-optical studies*

The MCD spectrum measured on a GO/$Fe_3O_4$ hybrid consists of contributions from the GO matrix and the $Fe_3O_4$ particles. Because the A-term is proportional to the derivative of the absorption band [2], a broad absorption tail also broadens the MCD lines. In a matrix with $E_U$ = 0.91 eV, strong overlap of the MCD lines associated with transitions of $Fe^{3+}$ and $Fe^{2+}$ ions at the A and B sites of $Fe_3O_4$ [3] is expected, as well as a signal at energies below $E_g$. For this reason $E_U$ is needed as a background parameter when decomposing the spectra into components.

Remeasuring $E_U$, $E_g$ and $I_D/I_G$ on GO/$Fe_3O_4$ samples makes it possible to distinguish the mechanisms listed in Table 4. An increase in $E_U$ would mean that the $Fe_3O_4$ particles introduce additional structural disorder into GO. A red shift of the absorption edge with unchanged $E_U$ would indicate restoration of sp² domains or charge transfer between GO and $Fe^{3+}$. The Raman ratio $I_D/I_G$

HSR (LONDON),
HOUGHTON STREET REVIEW JOURNAL
ISSN: 2058-5519|Impact factor-15.9
http://houghtonstreetreview.com/index.php/hsr

serves as an additional criterion for separating these two cases. The values obtained in this work serve as the reference point for such a comparison.

**Table 4.** Expected changes in GO/$Fe_3O_4$ samples and their interpretation

| Scenario | $E_U$ | $E_g$ | $I_D/I_G$ | Interpretation |
|---|---|---|---|---|
| Increased disorder | increases | unchanged or increases | increases | $Fe_3O_4$ introduces additional defects into GO |
| Partial reduction | unchanged | decreases | increases | $sp^2$ domains are restored |
| Charge transfer | unchanged | decreases | unchanged | electron exchange between GO and $Fe^{3+}$ |
| Simple mixture | unchanged | unchanged | unchanged | spectrum equals the sum of components |

### *4.4. Limitations*

The analysis was carried out on aqueous dispersions, so α represents the volume absorption of the dispersion. $E_U$, which is obtained from the slope, does not depend on this, whereas the absolute value of $\alpha_0$ depends on concentration. In thin films the scattering contribution is reduced and the results become closer to the sample geometry used in MCD measurements. The temperature dependence of $E_U$ and a series of samples with different degrees of oxidation will be studied in future work.

## 5. Conclusions

The optical absorption edge of GO synthesized by the Hummers method was analyzed comprehensively. The ln α versus hν dependence is linear over 2.00–3.45 eV ($R^2 = 0.9994$), and $E_U = 0.91 \pm 0.01$ eV, a value that does not depend on concentration and is only weakly sensitive to the choice of window. Model comparison showed that the exponential tail is preferable to the scattering model, but the obtained value should be interpreted as an effective disorder parameter. Tauc analysis gave fits of equal quality for n = 2 and n = 1/2, yielding 3.35 eV and 1.87 eV, respectively. The Raman-based $L_a = 1.16$ nm together with the Robertson–O'Reilly relation supports the n = 1/2 model. The values $E_U/E_g = 0.27$ and $\sigma = 0.028$ confirm the strong disorder of GO. The obtained $E_U$, $E_g$ and $L_a$ values are proposed as baseline parameters for interpreting MCD and Kerr spectra of GO/$Fe_3O_4$ hybrids, and a scheme for distinguishing the mechanisms (Table 4) is presented.

HSR (LONDON),
HOUGHTON STREET REVIEW JOURNAL
ISSN: 2058-5519|Impact factor-15.9
http://houghtonstreetreview.com/index.php/hsr

**References**

1. Zubir N.A., Yacou C., Motuzas J., Zhang X., Diniz da Costa J.C. Structural and functional investigation of graphene oxide–Fe3O4 nanocomposites for the heterogeneous Fenton-like reaction // Sci. Rep. 2014. Vol. 4. Art. 4594.
2. Stephens P.J. Magnetic circular dichroism // Annu. Rev. Phys. Chem. 1974. Vol. 25. P. 201–232.
3. Fontijn W.F.J., van der Zaag P.J., Devillers M.A.C., Brabers V.A.M., Metselaar R. Optical and magneto-optical polar Kerr spectra of Fe3O4 and Mg2+- or Al3+-substituted Fe3O4 // Phys. Rev. B. 1997. Vol. 56. P. 5432–5442.
4. Eda G., Lin Y.-Y., Mattevi C., Yamaguchi H., Chen H.-A., Chen I.-S., Chen C.-W., Chhowalla M. Blue photoluminescence from chemically derived graphene oxide // Adv. Mater. 2010. Vol. 22. P. 505–509.
5. Mathkar A., Tozier D., Cox P., Ong P., Galande C., Balakrishnan K., Reddy A.L.M., Ajayan P.M. Controlled, stepwise reduction and band gap manipulation of graphene oxide // J. Phys. Chem. Lett. 2012. Vol. 3. P. 986–991.
6. Tauc J., Grigorovici R., Vancu A. Optical properties and electronic structure of amorphous germanium // Phys. Status Solidi B. 1966. Vol. 15. P. 627–637.
7. Makuła P., Pacia M., Macyk W. How to correctly determine the band gap energy of modified semiconductor photocatalysts based on UV-Vis spectra // J. Phys. Chem. Lett. 2018. Vol. 9. P. 6814–6817.
8. Urbach F. The long-wavelength edge of photographic sensitivity and of the electronic absorption of solids // Phys. Rev. 1953. Vol. 92. P. 1324.
9. Cody G.D., Tiedje T., Abeles B., Brooks B., Goldstein Y. Disorder and the optical-absorption edge of hydrogenated amorphous silicon // Phys. Rev. Lett. 1981. Vol. 47. P. 1480–1483.
10. Studenyak I., Kranjčec M., Kurik M. Urbach rule in solid state physics // Int. J. Opt. Appl. 2014. Vol. 4, No. 3. P. 76–83.
11. Hummers W.S., Offeman R.E. Preparation of graphitic oxide // J. Am. Chem. Soc. 1958. Vol. 80. P. 1339.
12. Robertson J., O'Reilly E.P. Electronic and atomic structure of amorphous carbon // Phys. Rev. B. 1987. Vol. 35. P. 2946–2957.
13. Ferrari A.C., Robertson J. Interpretation of Raman spectra of disordered and amorphous carbon // Phys. Rev. B. 2000. Vol. 61. P. 14095–14107.
14. Tuinstra F., Koenig J.L. Raman spectrum of graphite // J. Chem. Phys. 1970. Vol. 53. P. 1126–1130.
15. Lai Q., Zhu S., Luo X., Zou M., Huang S. Ultraviolet-visible spectroscopy of graphene oxides // AIP Adv. 2012. Vol. 2. Art. 032146.
16. Krishnamoorthy K., Veerapandian M., Yun K., Kim S.-J. The chemical and structural analysis of graphene oxide with different degrees of oxidation // Carbon. 2013. Vol. 53. P. 38–49.
17. Dimiev A.M., Halbig C.E., Talyzin A. A critical review to avoid common misinterpretations in characterizing graphene oxide // Chem. Rev. 2026. Vol. 126. P. 3055–3088.